**Proceedings of the ASME 2009 Fluids Engineering Division Summer Meeting**
**FEDSM2009**
**August 2-6, 2009, Vail, Colorado USA**

# FEDSM2009-78283

## Motion of Liquid Drops through Complex 3D Clothing

**Hojjat Nasr**
Department of Mechanical and Aeronautical Engineering Clarkson University
Potsdam, NY 13699

**Goodarz Ahmadi**
Mechanical and Aeronautical Engineering Department, Clarkson University
Potsdam, NY 13699, USA
ahmadi@clarkson.edu

**Homan Tafreshi**
Department of Mechanical Engineering
Virginia Commonwealth University
PO Box 843015
Richmond, VA 23284

**John B. McLaughlin**
Department of Chemical and Biomolecular Engineering Clarkson University
Potsdam, NY 13699

### Abstract

This study was concerned with the numerical simulation of a moving drop through a fabric due to a wettability gradient. The wettability gradient was introduced by varying the contact angle along the staggered fibers of a fabric. The unsteady laminar Navier-Stokes equation was solved using a fixed Eulerian unstructured grid. The Volume of Fluid Model (VOF) was used to account for tracking the gas/liquid interface. A water drop was placed on top of the fabric with an initial velocity, and the motion of the drop through the fabric was studied. Several computer simulations under different conditions such as the distance between fibers, contact angle distribution, and drop initial velocity were performed, and the results were compared with each other. In order to verify the accuracy of the computational model, the motion of a drop on a surface due to a wettabily gradient was simulated as a benchmark.

### Introduction

There has been interest on controlling the motion of drops on solid surfaces due to the numerous applications such as, protective clothing, pharmaceutical applications, ink jet printers, and micro-fluidics devices. Generally, when a drop is placed on a surface, it deforms and spreads out until its shape is conformed to its contact angle on the surface. When there is a gradient of contact angle on the surface, in addition to the spreading, the drop will move.

The motion of drop on surfaces due to the wettability gradient was first identified by Greenspan (1978). Brochard (1989) studied the motion of droplets on solid surfaces induced by wettability and temperature gradient. Brochard also developed a theoretical model for the motion of two-dimensional ridges and spherical droplets due to the wettability gradient in the presence and in the absence of temperature gradient. She also concluded that there are mechanical forces due to the variation in the contact angle that makes the drop move. Subramanian et al. (2005) proposed two approximate analytical solutions for the motion of a drop on a solid surface due to the wettability gradient. One solution approximated the shape of the drop as a collection of wedges, and the other solution made use of lubrication theory. They reported that the results from wedge approximation and lubrication theory agreed at small contact angles (< 30).

Despite many experimental and analytical studies in this area, the available computer simulations of droplet motion due to wettability gradient are rather scarce. In this study, the wettability gradient in a fabric was introduced by varying the static contact angle of the cloth fibers. The unsteady Navier-Stokes equation was solved in both liquid and gas phases using the Volume of Fluid Model (VOF) on a fixed Eulerian unstructured grid. The VOF accounted for tracking the gas-liquid interface. The simulation results for a water drop with different initial velocities through a fabric were studied. To understand the effect of cloth fiber distances in the fabric on the motion of a droplet, two configurations of high and low concentration fabrics were studied.

## Nomenclature

| | |
|---|---|
| t | time (s) |
| $u_i$ | velocity ($ms^{-1}$) |
| p | pressure ($N\ m^{-2}$) |
| $h_0$ | ridge height (m) |
| R | ridge radius (m) |
| $x_{max}$ | macroscopic cutoff (m) |
| $x_{min}$ | molecular size (m) |

*Greek letters*

| | |
|---|---|
| $\rho$ | density ($Kg\ m^{-3}$) |
| $\mu$ | viscosity (Pa s) |
| $\alpha$ | volume fraction |
| $\theta$ | static contact angle |
| $\gamma$ | Surface tension ($N\ m^{-1}$) |

*Subscripts*

| | |
|---|---|
| q | local volume fraction of the $qth$ fluid |
| w | wall |

## Governing Equations

In the Volume of Fluid (VOF) approach a single momentum equation is solved throughout the computational domain, and the resulting velocity field is shared among the phases. In each computational cell the mass density and the viscosity $\rho$ and $\mu$ are evaluated depending on the volume fractions of all phases. The governing equations for the unsteady flow are given as:

Continuity:

$$\frac{\partial \rho}{\partial t} + \frac{\partial}{\partial x_i}(\rho u_i) = 0 \tag{1}$$

Momentum:

$$\frac{\partial}{\partial t}(\rho u_i) + u_j \frac{\partial}{\partial x_i}(\rho u_i) = \frac{\partial p}{\partial x_i} + \nu \nabla^2 u_i + F_{vol} \tag{2}$$

As noted before, the VOF technique is used to track the gas-liquid interface. According to the VOF model, phases are not interpenetrating. For each additional phase, a new variable that is the volume fraction of the phase in the computational cell is introduced. In each cell, the volume fractions of all phases must sum to unity. The fields for all variables and properties are shared by the phases and represent volume-averaged values, as long as the volume fraction of each of the phases is known at each location. Thus, the variables and properties in any given cell are either representative of one of the phases or a mixture of the phases, depending upon the volume fraction values. The volume fraction of the $qth$ phase, $\alpha_q$, satisfies the continuity equation:

$$\frac{\partial \alpha_q}{\partial t} + u_j \frac{\partial \alpha_q}{\partial x_j} = 0 \tag{3}$$

The volume fraction is subject to the following constraint:

$$\sum_{q=1}^{n} \alpha_q = 1 \tag{4}$$

Note that the volume fraction equation is not solved for the primary phase, but is evaluated from equation (4).

As noted before, various properties are evaluated based on the volume fraction weighted phase averages in each control volume. e.g., $\rho = \sum_{q=1}^{n} \alpha_q \rho_q$. The additional, the surface tension effect for the VOF calculation results in a source term in equation (2) and is expressed as a volume force given as

$$F_{vol} = \sigma_{ij} \frac{\rho k_i \nabla \alpha_i}{1/2(\rho_i + \rho_j)} \tag{5}$$

It is important to note that equation (5) is valid when two phases are present in each computational cell. The contact angle at the wall is given as $\theta_w$, and the unit normal to the cell next to the wall is given by

$$\hat{n} = \hat{n}_w \cos\theta_w + \hat{t}_w \sin\theta_w \tag{6}$$

The values for the contact angle at the wall are given as the boundary conditions; in this study a linear distribution for the contact angle is chosen.

## Simulation Results

To verify the accuracy of the present computational model, the motion of a droplet on a surface due to a wettabily gradient was first studied.

### Droplet Motion on a Surface

In this section, the simulation results for the motion of a droplet on a surface due to the wettability gradient are investigated. The wettability gradient is introduced by varying the static contact angle along the surface. Motion of water droplet is studied. The viscosity and surface tension of water are listed in Table 1. A linear distribution for the wettability gradient is used in these simulations. That is, the static contact angle varies linearly from $90^\circ$ at the beginning to $50^\circ$ at the end of the computational domain. Figure 1 shows the geometry and the initial position of the drop on the surface. A two dimensional cylindrical ridge is chosen to represent the droplet. The initial dynamic contact angle of the drop in the front and receding interface is taken to be $90^\circ$ which represents a half of a cylindrical ridge. The values of the parameters shown in figure 1 are listed in Table 1. Figure 2 shows the unstructured triangular grid used in the present computation. To avoid numerical diffusion associated with the approximate resolution of sharp interfaces, special care must be given to the grid generation.

**Table 1:** Water properties and geometry dimensions

| | |
|---|---|
| Viscosity $\mu$ | 0.001 Pa.s |
| Surface tension $\gamma$ | 0.072 N/m |
| $h_0$ | 1.33 mm |
| R. | 1.33 mm |
| L | 12 mm |

Brochard (1989) derived an expression for the velocity of a cylindrical ridge by balancing the driving force due to the wettability gradient and the viscous force. Accordingly,

$$U^{Brochard} = \frac{2\, h_0\, S'}{3\mu \ln(\frac{x_{max}}{x_{min}})} \qquad (7)$$

where $h_0$ is the height of the ridge at $t = 0$, $\mu$ is the dynamic viscosity of the liquid in the droplet, $x_{max}$ is a macroscopic cutoff ($x_{max} \sim R/2$), $x_{min}$ a molecular size ($x_{min} \sim 0.5\,nm$), and $S'$ is given as:

$$S' = -\gamma \frac{d\theta}{dx} \times \frac{\pi}{180} \qquad (8)$$

where $\gamma$ is the surface tension of drop liquid against ambient air, $\theta$ is the static contact angle in degree, and $\pi/180$ is a conversion factor from degree to radian. Subramanian et al. (2005) showed that the velocity predicted by Brochard is too large by a factor 2 (see Eqs. (14) and (15) of their paper and the subsequent discussion). The value for average velocity of the droplet according to corrected Brochard's analytical expression is 125 mm/sec, while for the present simulation the average droplet speed is about 160 mm/sec. Figure 3 shows the snap shots of droplet migration on the surface due to the wettability gradient. It is seen that as the drop moves on the surface, the contact angle of the drop decreases and the drop footprint increases. It is also observed from this figure that the front contact angle is less than the receding contact angle.

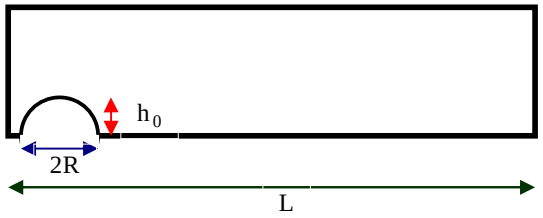


**Figure 1:** Schematics of the geometry and initial position of drop.

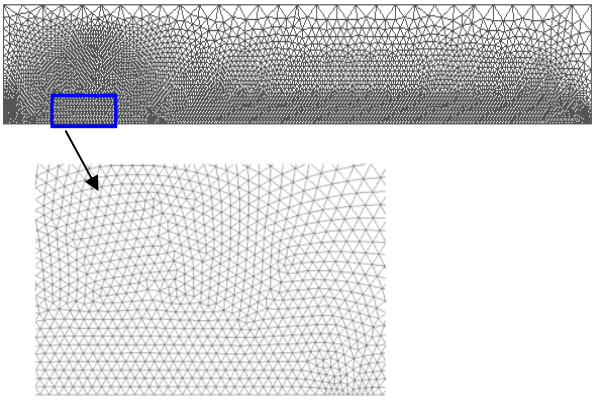

**Figure 2:** Computational domain for studying the motion of droplet on a surface.

### Droplet Motion through a Fabric

In this section, the computer simulation for the motion of a droplet through a fabric is studied. Figure 4 shows two configurations used in the present study. In both cases the fiber diameter is 20 $\mu m$. In the less dense fabric concentration, the horizontal and vertical distances between the center of fibers are, respectively, 70 and 35 $\mu m$, while in concentrated fabric configuration, these values are 40 and 20 $\mu m$. The initial location of drop is shown in this figure. The droplet diameter is typically 140 $\mu m$ with its thermophysical properties listed in Table 1.

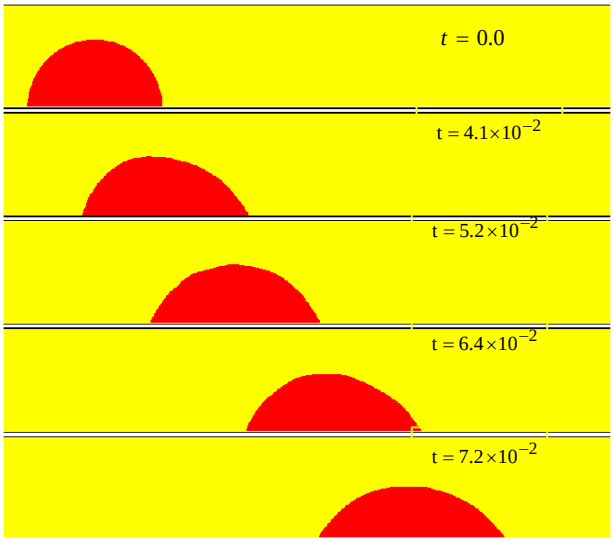


**Figure 3:** Drop position at different times.

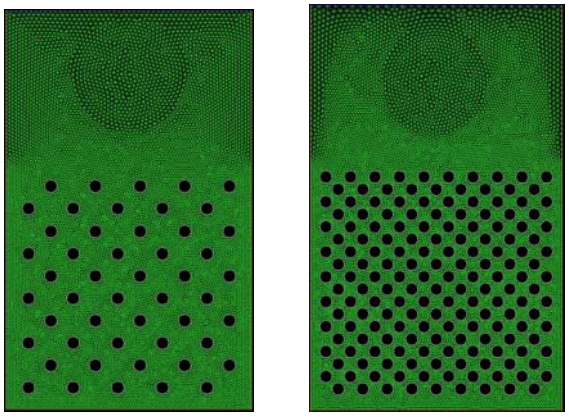

**Figure 4:** Schematics of the geometry and initial position of droplet.

The final location of the droplet for less concentrated fibers in the cloth is shown in Figures 5. The initial drop velocity is assumed to be 2 m/s. The static contact angle is ninety degrees in Figure 5a and zero degrees in Figure 5b, while in Figure 5c the contact angle changes linearly from ninety (the first row) to zero degrees (the last row). It is observed that when the static contact angle is zero degrees, maximum droplet penetration through the fabric is achieved. To study the effect of droplet initial velocity on its motion through the fabric, simulations are repeated using a higher initial velocity equal to 4 m/s. It is observed in Figure 6 that as the drop initial velocity increases, the droplet penetrates deeper into the fabric.

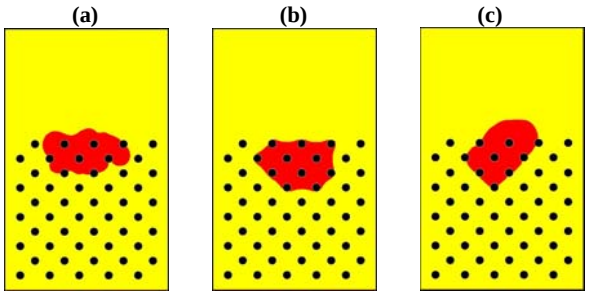


**Figure 5:** Final location of drop for less concentrated fibers; the initial drop velocity is 2 m/s. (a) $\theta_w = 90^\circ$ (b) $\theta_w = 0^\circ$ (c) $\theta_w = 90^\circ \rightarrow 0^\circ$.

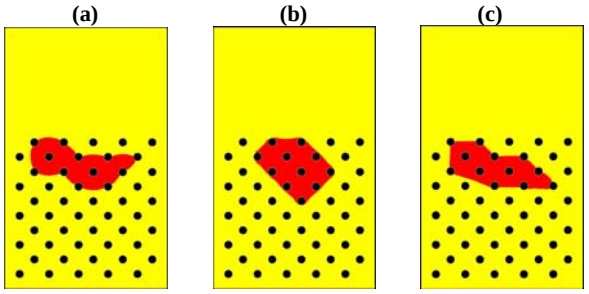


**Figure 6:** Final location of drop for less concentrated fibers; the initial drop velocity is 4 m/s. (a) $\theta_w = 90^\circ$ (b) $\theta_w = 0^\circ$ (c) $\theta_w = 90^\circ \rightarrow 0^\circ$.

The final location of the drop for highly concentrated fibers is shown in Figure 7. The initial droplet velocity is assumed 2 m /s. The static contact angle is ninety degrees in Figure 7a and zero degrees in Figure 7b, while in Figure 7c it changes linearly from ninety (the first row) to five degrees (the last row).
It is seen that the droplet cannot penetrate through the fabric when the contact angle is ninety degrees, but penetrates deeper when the contact angle is small. It is also seen, increasing the fiber concentration causes more penetration when the contact angle is small and causes less penetration when the contact angle is large.

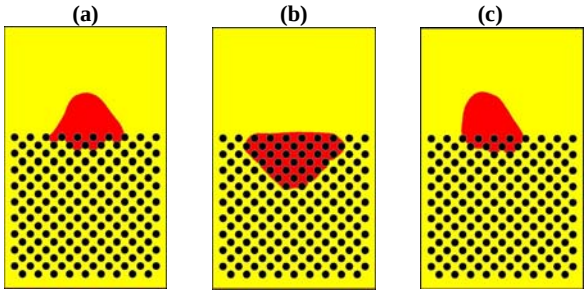


**Figure 7:** Final location of drop for highly concentrated fibers; the initial drop velocity is 2 m/s. (a) $\theta_w = 90^\circ$ (b) $\theta_w = 0^\circ$ (c) $\theta_w = 90^\circ \rightarrow 5^\circ$.

## Conclusions

Computer simulations of a moving drop on a surface and through a fabric due to wettability gradient under different conditions were performed. The unsteady laminar Navier-Stokes equation was solved using the Volume of Fluid Model (VOF) model on fixed Eulerian unstructured grid. On the basis of the presented results, the following conclusions may be drawn:

- As the water droplet moves on the surface, its footprint increases.
- When the static contact angle is zero degrees, the maximum droplet penetration through the fabric is achieved.
- Increasing the fiber concentration in the fabric causes more penetration through the fabric when the contact angle is small but leads to less penetration when the contact angle is large.

## Acknowledgment

The financial support Army Research Office (ARO) is gratefully acknowledged.

## References

Brochard, F., Motions of Droplets on Solid Surfaces Induced by Chemical or Thermal Gradients, Langmuir, 5, 432, (1989).

Greenspan, H. P., J. Fluid Mech., Vol. 84,125, (1978).

Subramanian, R. S, Moumen, N. & Mclaughlin, J. B., Motion of Drop on Solid Surface Due to a Wettability Gradient, Langmuir, Vol. 21, 11844-11849, (2005).